Numerical modelling of Cone Penetration Test in Clay using Coupled Eulerian Lagrangian Method

Fallah, Sogol; Gavin, Kenneth; Jalilvand, Soroosh

Publication date
2016

Document Version
Final published version

Published in
Proceedings of Civil Engineering Research in Ireland 2016

Numerical modelling of Cone Penetration Test in Clay using Coupled Eulerian Lagrangian Method

Sogol Fallah [1], Kenneth Gavin[2], Soroosh Jalilvand[3]
[1] Arup, 50 Ringsend Rd, Dublin 4, Ireland (Formerly UCD)
[2] Delft University of Technology, Department of Geoscience and Engineering, Delft, Zuid-Holland, Netherlands (Formerly UCD)
[3] School of Civil Engineering, University College Dublin, Newstead, Belfield, Dublin 4, Ireland
email: sogol.fallah@arup.com , K.G.Gavin@tudelft.nl, soroosh.jalilvand@ucdconnect.ie

ABSTRACT: The Cone Penetration Test (CPT) has been extensively used in geotechnical engineering, to evaluate the properties of wide range of soils. Numerical simulations of CPT involves large deformations in the soil domain which causes numerical difficulties in traditional finite element analysis. Early numerical studies used simplifying assumptions such as wished-in-place condition and in-situ stress distribution as the initial stress state of the soil domain. Recent developments in finite element analysis allow large deformation analyses to be performed.
This paper presents the results of the continuous penetration of cone in single-layer and double-layer clay using the Coupled Eulerian Lagrangian (CEL) method. Performance of the CEL technique in modelling the cone penetration test was validated against the existing studies. Then, a parametric study was performed to develop a correlation between the cone bearing factor and rigidity index of the clay. The proposed correlation showed a very good agreement with the existing experimental and numerical correlations. The cone penetration test in double-layer clay was simulated. The results suggested that CEL analysis is a reliable technique in modelling large deformation problem of cone penetration test.

KEY WORDS: Large Deformation Finite Element Analysis; Cone Penetration Test; Eulerian Analysis.

1 INTRODUCTION

The Cone Penetration Test (CPT) is one of the most widely utilised in-situ tests used common to evaluate the properties of soil. It is widely used at both onshore and offshore sites due its applicability in a wide range of soil types. The cone tip end resistance, q_c profile obtained from the test is a good representative of engineering properties of the soil. The resistance provided by the cone tip can be represented by cone factor, $N_c = q_c/s_u$. Different studies have aimed to stimulate the cone resistance by developing correlations between N_C and soil properties [1]–[4].

Many researchers have used numerical analysis to investigate the mechanisms controlling the cone tip resistance during penetration [5]–[11]. Because of the numerical difficulties associated with performing large deformation analyses, early work on finite element analysis of cone penetration test assumed the cone to be wished-in-place with simplifying assumptions of original in-situ stress field around the cone.

This paper presents the results of an advanced technique in finite element analysis in modelling large deformation problems. Coupled Eulerian Lagrangian technique was used to simulate the continuous penetration of the cone in single-layer and double-layer clay. The results were compared with existing experimental and numerical studies and showed a very good agreement.

2 COUPLED EULERIAN LAGRANGIAN TECHNIQUE

When performing large deformation problems excessive mesh distortions may lead to difficulty with convergence or inaccurate results during numerical modelling. To overcome these problems, different techniques have been introduced such as Arbitrary Lagrangian-Eulerian (ALE) and Coupled Eulerian Lagrangian (CEL) techniques. The ALE technique aims to reduce the distortions by remeshing the domain at a certain frequency. The field values are interpolated and transferred from the old mesh to a new improved mesh. In this method, the number of elements and the connectivity of the nodes do not change during the remeshing process. Instead the nodes are moved to find a new position in order to reduce the distortion of elements.

The Coupled Eulerian Lagrangian (CEL) method provides an environment in which both Lagrangian and Eulerian materials can be used. The difference between the Lagrangian and Eulerian approaches in finite element analysis is illustrated in Figure 1. In the traditional Lagrangian approach, shown in Figure 1 (a), the elements are filled with material and they deform as the material deforms. In the Eulerian approach, the elements are fixed and the material flows through the elements as shown in Figure 1 (b). As a result, there is no mesh distortion in the Eulerian approach. As shown in Figure 1 (b), multiple materials can exist in an Eulerian element.

This method of analysis avoids excessive mesh distortions although it has limitation on defining the material boundaries. Since the boundaries between the materials are approximate, the boundary surface may be discontinuous in this approach.

The reliability of CEL method in large deformation analysis has been addressed in recent researches on different types of geotechnical problems [12]–[17]. Qiu et al. (2011) investigated the capabilities of the CEL method by simulating pile installation and the effects of a ship running aground at an embankment [12]. The results showed good agreement with

classic finite element method and in-situ measurements. Tho et al. (2012, 2013) performed three dimensional Eulerian analyses to investigate the pentration of jack-up foundation, known as spudcan and assessed the effect of spudcan penetration on adjacent piles ([16], [17]). The results were compared to experimental data from a centrifuge test and a good agreement was obtained. The above studies suggest that the CEL technique is a reliable approach to solve large deformation problems such as spudcan installation. Consequently, the CEL method was adopted in this study.

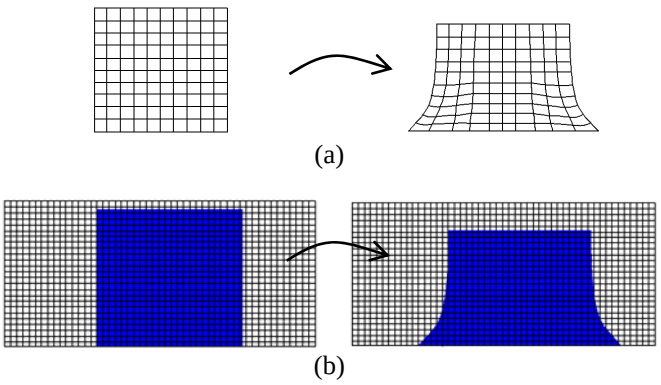

Figure 1. Lagrangian Vs Eulerian technique

The CEL method is implemented in Abaqus/Explicit [18]. In the explicit integration scheme the unknown solution for the next time step can be found directly from the solution of the previous time step, such that no iteration is required. Explicit calculations are not unconditionally stable. The numerical stability in the CEL analysis is guaranteed by introducing the critical time step size Δt_{crit} as following [18],

$$\Delta t_{crit} = \frac{L_e}{c_d} \quad (1)$$

Where L_e is the characteristic element length and Δt_{crit} is the critical time step.

2.1 *Contact formulation in CEL technique*

The implementation of Eulerian-Lagrangian contact is an extension of general contact in Abaqus/Explicit [18]. The contact interface is automatically identified between the Lagrangian structure and Eulerian elements so there is no need to generate a conforming mesh for the Eulerian domain. As the Lagrangian structure passes through Eulerian elements, the material is pushed out of the Eulerian elements. Similarly, the Eulerian material is prevented from flowing into the elements occupied by Lagrangian structure in order to ensure that two materials never occupy the same physical space. A layer of void Eulerian elements must be defined at the free surface to provide space for replaced Eulerian material that is driven out of the interior elements. This will be discussed in the following sections. In this study the tangential contact was considered to be frictionless.

3 CEL ANALYSIS OF CONE PENETRATION TEST

3.1 *Validation*

The accuracy of the present study was confirmed by comparing the results of analysis to existing numerical modelling. Zheng et al. (2013) presented the results of the analysis of cone penetration into a single-layer of weightless clay with a rigidity index, $I_R = G/s_u = 100$ [19]. The material had an undrained shear strength of 10 kPa and poison's ratio of 0.495.

The finite element model used for this analysis is shown in Figure 2. The domain was 7.5D wide and 7D in depth additional to penetration depth of 12D, where D is the diameter of the cone. The mesh was refined around the region where the cone was penetrating, whilst a coarser mesh was adopted remote from the cone in order to optimize computing resources for analyses. A total number of 2,604,960 elements were included in the domain. The time required for this analysis was about 78 hours using the Fionn supercomputer at the Irish Centre for High-End Computing (ICHEC) that provides 24 cores with 2.4GHz Intel processors. A penetration rate of (D/10) /s was selected to assure the quasi-static conditions during the analysis.

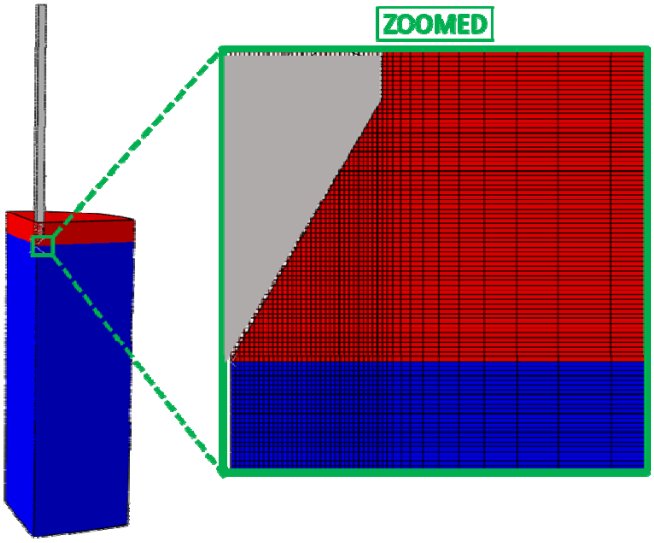

Figure 2. Finite element model of cone penetration analysis

Figure 3 shows the comparison of the results of cone penetration into the single-layer weightless soil from this study with the response predicted by Walker and Yu (2006) [20]. The vertical axis shows the normalised vertical displacement u/D. The displacement was considered zero when the maximum cross section of the cone entered the seabed. The load-penetration curves, the depth at which the cone reaches its steady state penetration resistance and the final penetration resistance were very well captured. The effect on the cone factor of the soils rigidity index will be discussed later in this paper and the results will be compared to the literature for further validation.

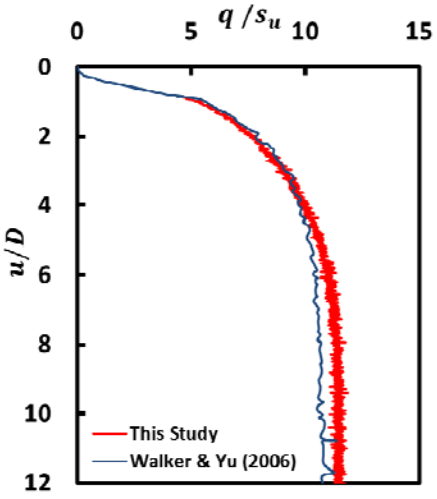

Figure 3. Comparison of penetration resistance in single-layer clay from this study and Walker and Yu (2006)

3.2 Effect of rigidity Index

The CEL analysis of a CPT with a standard cone angle of 60° was undertaken in clay with rigidity index in the range of 25 to 300. The soil was considered as weightless with uniform shear strength profile with depth. The maximum penetration depth considered was 14 times cone diameter (D_c) which allowed the cone resistance to reach the steady state that is the representative value for the cone factor.

The cone-soil interaction was considered frictionless and sliding is allowed at the soil-cone interface. Figure 4 shows the evolution of the cone resistance as the cone penetrometer was pushed into weightless uniform clay obeying the Tresca failure criterion. It can be concluded from Figure 4, that it is not necessary to continue the analyses beyond a penetration depth of 8 diameters as a steady state condition had been reached for all values of rigidity index.

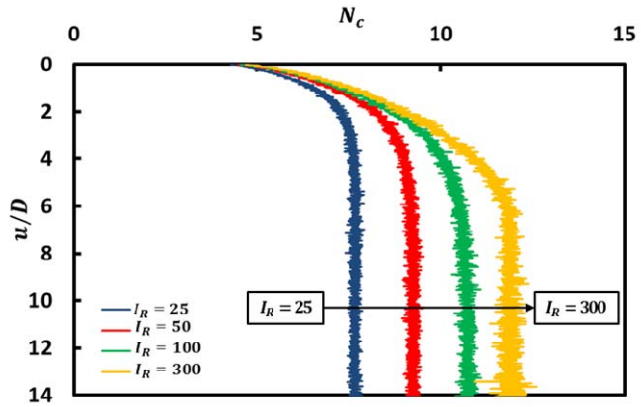

Figure 4. Variation of normalised bearing capacity with normalised depth for cone penetration in uniform clay with different rigidity index values

Figure 4 indicates that the required depth to achieve a steady state condition increased with rigidity index. These results show that a steady state condition is achieved after a penetration depth of approximately 4 cone diameters in a Tresca material with $I_R = 25$, whilst a penetration depth of approximately 8 cone diameters is required for a material with $I_R = 300$.

The variation of steady state cone with rigidity index is plotted on a logarithmic scale and Figure 5. The equation shown is a numerical fit to the achieved data. This is validated against the existing correlation in literature as shown in Figure 6. It can be seen that the result obtained cone factors using the proposed correlation agrees well with the previous studies. Table 1 summarises the numerical values obtained.

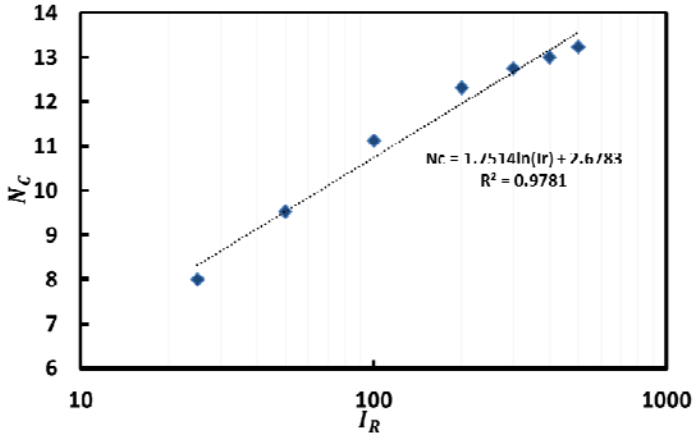

Figure 5. Variation of cone factor with rigidity index

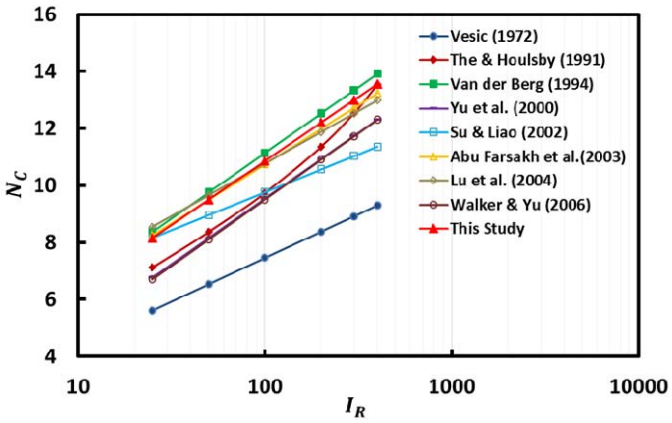

Figure 6. Comparison of cone factor from this study to literature

During deep penetration, the plastic zone is confined by elastically deforming soil. The extent of the plastic zone depends on the soil rigidity index. The results of the simulations were further verified by assessing of the plastic zone at different penetration depths. The distribution of the plastic zone at penetration depths of 1D, 3D, 5D, 7D, 9D, 11D, 13D and 15D are plotted and shown in Figure 7.

Table 1. Comparison of cone factor from this study to literature

I_R	25	50	100	300
Vesic (1972)	5.61	6.53	7.45	8.92
Teh and Houlsby (1991)	7.12	8.37	9.73	12.54
Van der Berg (1994)	8.37	9.75	11.14	13.34
Yu et al. (2000)	6.77	8.15	9.54	11.74
Su and Liao (2001)	8.16	8.96	9.76	11.03
Abu-Farsakh et al. (2003)	8.24	9.49	10.74	12.72
Lu et al. (2004)	8.55	9.66	10.77	12.53
Walker and Yu (2006)	6.70	8.10	9.50	11.72
This Study	7.94	9.12	10.29	12.16

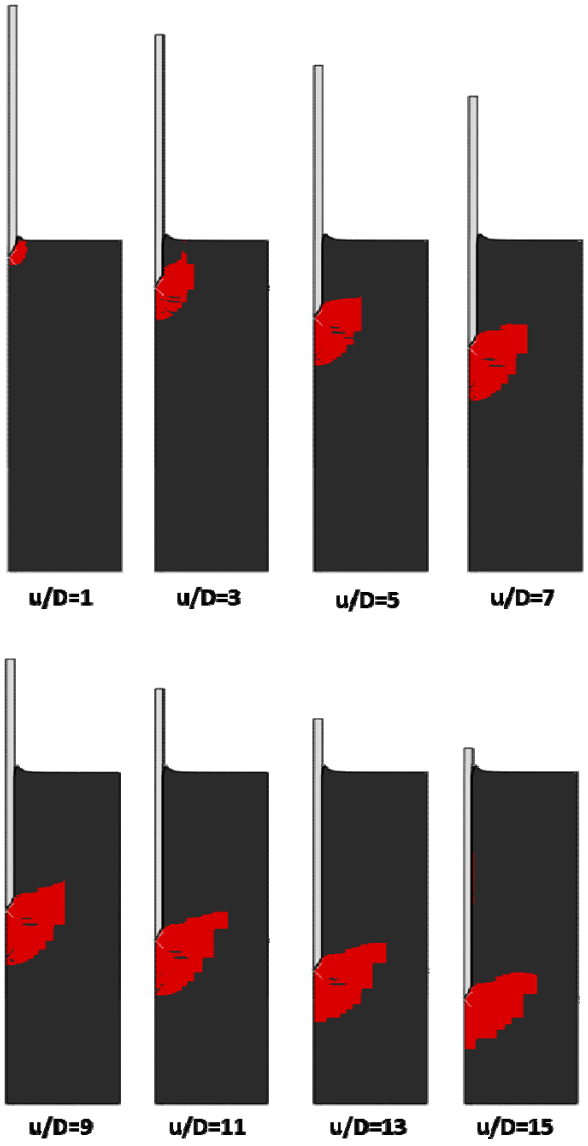

Figure 7. Plastic zone at different penetration depths

As seen in Figure 7 the border between the elastic and plastic zones is not smooth. This discontinuity occurs in the Eulerian mesh due inaccuracies in defining the material interface for the Eulerian elements, as explained earlier. Since the mesh becomes coarser as the distance from the cone increases, the material discontinuity in the elements is more apparent for deeper penetrations. The discontinuity at the material interface definition did not affect the cone resistance profile. Figure 7 indicates that the size of plastic zone did not change after u/D=7, which shows the development of the local failure mechanism.

Teh and Houlsby (1991) reviewed previous studies on semi-analytical approaches to estimate cone resistance [22]. They concluded that the approaches used for the bearing capacity of shallow penetration are inappropriate for deep penetration. The shallow failure mechanism extends to the free surface while the deep failure mechanism is localized (confined) around the penetrating object. As the cone penetrates into the soil, the plastic zone that is surrounded by elastic soil moves deeper into the ground. This transition can occur at penetrations at a normalized depth of 2–3 diameters in homogeneous soil [26]. The results from this study illustrated in Figure 7 also shows that the plastic zone does not extend to the surface in cone penetration test and therefore the mechanism is different for shallow and deep penetration.

The size of the plastic region varies with the rigidity index of the soil, I_R. Lu et al. (2004) showed that the stress contours are formed around a centre, O, that is located at the distance equal to one radius of the penetrometer, R, below the maximum cross section of the penetrometer as illustrated in Figure 8 [9]. Variation of the radius of the plastic zone, R_p, and depth of the plastic zone Z_p with rigidity index of the soil is also shown in this figure. Figure 9 shows the plastic zone developed around the penetrometer tip for different values of rigidity index.

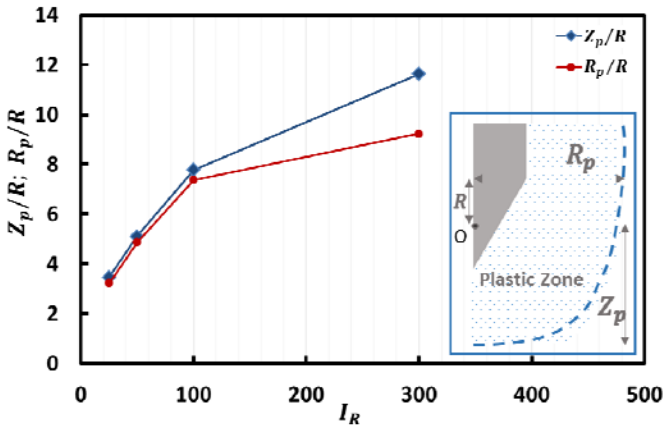

Figure 8. Variation of plastic zone extent with rigidity index of the soil

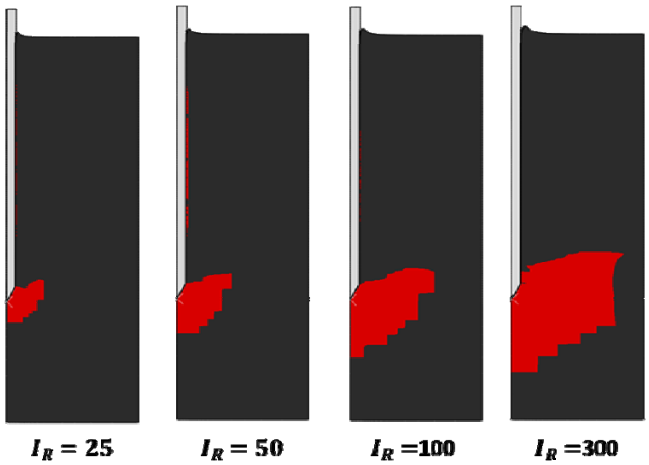

Figure 9. Plastic zones at steady state condition for different values of rigidity index of the soil

4 SIMULATION OF CONE PENETRATION IN DOUBLE-LAYER CLAY

Having validated the CEL technique in modelling cone penetration in a single layer clay, the performance of this method was assessed in simulating the cone penetration in a double-layer clay. A comparison was made between the results of this study and a numerical analysis previously conducted by Walker and Yu (2010) [11].

For the sake of consistency, the soil was modelled as a weightless undrained clay with elastic perfectly plastic behaviour. The shear modulus is selected as $G = 1 MPa$ and the Poisson ratio is set to 0.49 for both the top and bottom layers. The rigidity index of the top and bottom layers are chosen as 100 and 300, respectively. Moreover, the top layer depth was taken as 8.4 times the diameter of the cone. The simulation continued until a penetration depth of 15 times the cone diameter was achieved. Walker and Yu (2010) modelled the soil using axisymmetry while a 3D model was employed in this study [11]. The use of 3D model is a constraint of the available implementation of Coupled Eulerian Lagrangian technique.

Figure 10 shows the result of the normalized bearing capacities (q/s_{u2}) in terms of the normalized penetration depth (u/D) as obtained from this study (dots) and Walker and Yu (2010) [11] (solid lines). The results are reported for both single-layer (single value of rigidity index $I_R = 100$) and double-layer cases (rigidity indices of 100 and 300 for the top and bottom layers respectively). The single layer soil was treated as a double-layer soil with equal rigidity indices for the top and bottom layers [11]. The subset in Figure 10 shows the deformation of the bottom layer as the cone tip reaches the penetration depth of 8.4 times the cone diameter (the location of the bottom layer was equivalent to $u/D = 7.5$) in the double-layer case. The deformation in the bottom layer is exaggerated for the purpose of clarity. The interface of the top and bottom layers is demonstrated in Figure 10 with a horizontal line that passes through $u/D = 7.5$.

Comparison of the numerical results from CEL analysis in this study and the numerical results from ALE analysis by Walker and Yu (2010) [11] in Figure 10, suggests that the CEL technique provides smoother profile of bearing capacity, specifically at the interface of soft and stiff clay. This can be important when assessing the risk of punch-through problem in penetration of large offshore foundations such as spudcan.

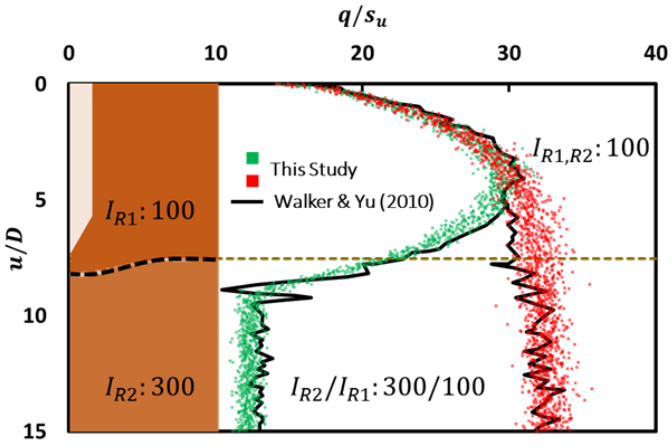

Figure 10. Comparison of the cone penetration results in double-layer clay to Walker and Yu (2010) [11].

5 SUMMARY AND CONCLUSION

This paper presented the results of large deformation analysis of cone penetration test in single-layer and double-layer clay. The coupled Lagrangian Eulerian technique was used for simulation of CPT in Abaqus/Explicit programme.

The cone resistance profile obtained from CEL analysis was validated against other numerical studies that were performed using the ALE technique. The results showed a very good agreement. A correlation was proposed to estimate the cone factor based on CEL analyses of CPT's in weightless soil with different values of rigidity index. The comparison of the proposed correlation with existing experimental and numerical correlations in the literature. The evolution plastic zone in the soil domain was also examined as the cone penetrated into the ground. The general pattern showed a good agreement with literature.

Finally, the cone penetration in double-layer clay was simulated and compared to other numerical studies. The results showed a very good agreement. The bearing capacity profiles from CEL analysis was found to be smoother that the AEL predictions and was deemed to be more realistic. This suggests that CEL can be a very good tool in predicting the potential of punch-through failure for example

REFERENCES

[1] Abaqus 6.13-2, V. (2013). "Abaqus v6.13 documentation, 2013." *Dassault Systèmes, Providence, RI, USA.*

[2] Abu-Farsakh, M., Tumay, M., and Voyiadjis, G. (2003). "Numerical Parametric Study of Piezocone Penetration Test in Clays." *International Journal of Geomechanics*, 1–12.

[3] Ahmadi, M. M., Byrne, P. M., and Campanella, R. G. (2005). "Cone tip resistance in sand: modeling, verification, and applications." *Canadian*

Geotechnical Journal, NRC Research Press Ottawa, Canada, 42(4), 977–993.

[4] Van der Berg, P. (1994). "Analysis of soil penetration."

[5] Dutta, S., Hawlader, B., and Phillips, R. (2012). "Finite Element Modeling of Vertical Penetration of Offshore Pipelines using Coupled Eulerian Lagrangian Approach." *Proceedings of the Twenty-second (2012) International Offshore and Polar Engineering Conference*.

[6] Hu, Y., Randolph, M. F., and Watson, P. G. (1999). "Bearing response of skirted foundation on nonhomogeneous soil." *Journal of geotechnical and geoenvironmental engineering*, American Society of Civil Engineers, 125(11), 924–935.

[7] Liyanapathirana, D. S. (2009). "Arbitrary Lagrangian Eulerian based finite element analysis of cone penetration in soft clay." *Computers and Geotechnics*, Elsevier Ltd, 36(5), 851–860.

[8] Lu, Q., Hu, Y., Randolph, M. F., and Bugarski, I. C. (2004). "A numerical study of cone penetration in clay." *Géotechnique*, Thomas Telford, 54(4), 257–267.

[9] Mayne, P. W., and Rix, G. J. (1993). "Gmax-qc Relationships for Clays." *Geotechnical Testing Journal, GTJODJ*, 16(1), 54–60.

[10] Pucker, T., and Grabe, J. (2012). "Numerical simulation of the installation process of full displacement piles." *Computers and Geotechnics*, 45, 93–106.

[11] Qiu, G., and Henke, S. (2011). "Controlled installation of spudcan foundations on loose sand overlying weak clay." *Marine Structures*, Elsevier Ltd, 24(4), 528–550.

[12] Qiu, G., Henke, S., and Grabe, J. (2011). "Application of a Coupled Eulerian–Lagrangian approach on geomechanical problems involving large deformations." *Computers and Geotechnics*, Elsevier Ltd, 38(1), 30–39.

[13] Robertson, P. K. (1990). "Soil classification using the cone penetration test." *Canadian Geotechnical Journal*, NRC Research Press, 27(1), 151–158.

[14] Robertson, P. K. (2009). "Interpretation of cone penetration tests-a unified approach." *Canadian Geotechnical Journal*, NRC Research Press, 46(11), 1337–1355.

[15] Robertson, P. K., and Wride, C. E. (1998). "Evaluating cyclic liquefaction potential using the cone penetration test." *Canadian Geotechnical Journal*, NRC Research Press, 35(3), 442–459.

[16] Su, S., and Liao, H. (2001). "Cavity expansion and cone penetration resistance in anisotropic clay." *Journal of the Chinese Institute of Engineers*, (July 2012), 37–41.

[17] Teh, C., and Houlsby, G. (1991). "An analytical study of the cone penetration test in clay." *Geotechnique*, (3), 529–532.

[18] Tho, K. K., Leung, C. F., Chow, Y. K., and Swaddiwudhipong, S. (2012). "Eulerian finite-element technique for analysis of jack-up spudcan penetration." *International journal of geomechanics*, 12(February), 64–73.

[19] Tho, K. K., Leung, C. F., Chow, Y. K., and Swaddiwudhipong, S. (2013). "Eulerian finite element simulation of spudcan–pile interaction." *Canadian Geotechnical Journal*, 50(6), 595–608.

[20] Tolooiyan, a., and Gavin, K. (2011). "Modelling the Cone Penetration Test in sand using Cavity Expansion and Arbitrary Lagrangian Eulerian Finite Element Methods." *Computers and Geotechnics*, Elsevier Ltd, 38(4), 482–490.

[21] Vesic, A. (1972). "Expansion of cavities in infinite soil mass." *Journal of Soil Mechanics & Foundations Div*.

[22] Walker, J., and Yu, H. (2010). "Analysis of the cone penetration test in layered clay." *Géotechnique*.

[23] Walker, J., and Yu, H. S. (2006). "Adaptive finite element analysis of cone penetration in clay." *Acta Geotechnica*, 1(1), 43–57.

[24] Yi, J., Goh, S., Lee, F., and Randolph, M. (2012). "A numerical study of cone penetration in fine-grained soils allowing for consolidation effects." *Géotechnique*, (2012), 707–719.

[25] Yu, H. S., Herrmann, L. R., and Boulanger, R. W. (2000). "Analysis of Steady Cone Penetration in Clay." *Journal of Geotechnical and Geoenvironmental Engineering*, American Society of Civil Engineers, 126(7), 594–605.

[26] Zheng, J., Hossain, M., and Wang, D. (2013). "3D large deformation FE analysis of spudcan and cone penetration on three-layer clays." *Twenty-third (2013) International Offshore and Polar Engineering*, 9, 453–460.